The effect of manufacturing flaws in the meso-structure of cast glass on the structural performance

Bristogianni, Telesilla; Oikonomopoulou, Faidra; Veer, Fred; Nijsse, Rob

DOI
10.1201/9780429426506-294

Publication date
2019

Document Version
Accepted author manuscript

Published in
Advances in Engineering Materials, Structures and Systems: Innovations, Mechanics and Applications

The effect of manufacturing flaws in the meso-structure of cast glass on the structural performance

T. Bristogianni & R. Nijsse
TU Delft, Civil Engineering and Geosciences, Netherlands

F. Oikonomopoulou & F. Veer
TU Delft, Faculty of Architecture, Netherlands

ABSTRACT: The success of projects such as the Crystal Houses façade in Amsterdam has triggered an increasing interest from architects, engineers and glass producers in the development and application of structural cast glass components. This interest raises, simultaneously, the needs for a controlled manufacturing process, a system for quality control and structural validation, to guarantee the production of safe components. Manufacturing-related flaws, such as stones, cord inclusions, or air-bubbles, occurring in the meso-structure of the components, form weak zones within the material and may lead to "spontaneous" cracking. The casting parameters such as the forming temperature and corresponding glass viscosity, the dwell time at this temperature and the cooling rate, largely determine the homogeneity of the final product. Additional complexity arises once the use of waste/recycled glass is considered, due to the probable presence of variable glass compositions and miscellaneous contaminants in the initial batch. The risk of inhomogeneity and resulting eventual mechanical failure, indicates the necessity of understanding the causes of flaw-formation and the impact of the developed flaws on the structural performance of the cast components. Therefore, a series of 50mm cubic glass components are cast at the TU Delft Glass Lab, using a selection of already formulated discarded soda-lime glasses from different commercial applications. The cubes' meso-structure is documented and- when required- scanned employing a Computer Tomography scanner and a polariscope to identify possible density differentials and internal stresses respectively. Then the cubes are tested for splitting strength and their performance is analyzed in relation to the previously documented flaws. The destructive tests suggest that there is a correlation between the meso-structure, structural performance and failure pattern of the cast glass components.

1 INTRODUCTION

Glass casting technology presents great potential for the building industry, which structural engineers and architects have only recently started to grasp. By casting, we can obtain structural glass elements of a considerable cross-section and a vast variety of envisioned shapes, colours, textures and opacities. All-glass load-bearing structures employing such elements- as the Crystal Houses façade in Amsterdam for example - combine robustness and unique aesthetics, while overcoming the inevitable challenges of a pioneering project (Oikonomopoulou et al. 2017). A current implication is the often empirical and manual production of cast glass in comparison to the mature, automated float glass production line, which can lead to product inconsistency and "spontaneous" failure. Therefore, as the interest in this type of structures increases, it becomes necessary to establish manufacturing and quality control standards, to guarantee a structurally sound product. This is specifically crucial once we consider- in the context of sustainability- waste glass as a raw source. In that direction, the Re^3 Glass project (TU Delft 2018) developed by the authors explores the possibilities and risks of waste glass recycling and repurposing in the building industry. Part of this research is presented in the paper, with the aim to highlight the occurrence of inhomogeneities and flaws in the mesostructure of the recycled cast glass components, and question their impact on the components' mechanical strength. The paper focuses in specific in the recycling of soda-lime float glass, given that the flat glass industry covers 29% of the glass production in the European Union (Glass Alliance Europe 2018) and consequently is responsible for a considerable waste stream. The discarded flat glass products are often downgraded or landfilled as their contamination from coatings or adhesives render them unsuitable for close loop recycling. Therefore, different float glass samples are cast at the TU Delft Glass Lab, in order to investigate if the encountered contaminations are critical for the production of cast glass building components. As a reference, specimens are also cast using soda-lime container glass cullet, as provided by the recycling industry. Given that the container glass sorting and recycling is at an advanced stage, it is interesting to compare the container cullet quality to that of the flat glass cullet.

2 GLASS DEFECTS

2.1 *Overview*

Bartuška (2008) groups the defects in the glass matrix in three main categories:

A. Crystalline inclusions
B. Glassy inhomogeneities (cord/ream)
C. Gaseous inhomogeneities (bubbles)

The level of contamination in the cullet will determine the type of defects to be expected in the recycled product. Cullet contamination is often categorized as (Vieitez et al. 2019):

a. Organics (e.g. plastic, textiles)
b. Non-glass inorganics (ceramics, stones, porcelain, glass ceramics)
c. Metals
d. Hazards
e. Different glass types (e.g. borosilicate, lead glass)

In our case, we choose to kiln-cast using only cullet, without the addition of new raw material. In this manner glass is formed at temperatures 400-500^{o}C lower than those required by the float and containers manufacturers, achieving significant energy savings and a considerable CO_2 reduction. However, the lower temperatures/ higher glass viscosities, in combination with the absence of pure batch, can intensify the presence of flaws. The size and shape of the cullet is also governing at such high viscosities (η= log3 to log4 in dPas) the level of inhomogeneities in the cast samples. Nonetheless, cast glass can tolerate more flaws than float or container glass products (Bristogianni et al. 2018) due to its considerable cross section and the different applied aesthetic criteria. Aim is to identify the type and quantity of acceptable defects before the integrity and mechanical properties of the cast structural component is compromised.

2.2 *Examined glass samples*

Different commercial float glass products were chosen for this study, covering a range of contaminants. The contamination source is organized as:

i. Coatings (soft, hard, mirror, frit)
ii. Variations in the float glass recipe (different manufacturer, tints)
iii. External contaminants during sorting (see section 2.1)

Figure 1 presents the studied samples (float and container glass) and their corresponding cullet size and contaminants. The relevant contaminant source (i-iii) and specific contaminant category (a-e) are also noted in this figure.

Float glass			
Type	**1. Fully tempered**	**2. Low-iron**	**3. Soft-coating**
Provided by	IFS-SGT	Cricursa	Pilkington
Cullet size	≈30*30*10mm	50*50*8mm	50*50*6mm
			
Cullet contamination	Clean	Clean	i) Coating: high percentage of ZnO
Type	**4. Hard-coating**	**5. Mirror 1**	**6. Mirror 2**
Provided by	Pilkington	-	-
Cullet size	50*50*4mm	50*50*3mm	50*50*3mm
			
Cullet contamination	i) Coating: high percentage of SnO2	i) Dialectric coating: BaO, ZnO, MgO, S, TiO2. Reflective coating: ZnO, MgO, Fe2O3, Ag2O	i) Dialectric coating: BaO, TiO2, MgO, S, ZnO, Fe2O3. Reflective coating: ZnO, MgO, Fe2O3, Ag2O
Type	**7. Auto windshield**	**8. Tint, coat, clear**	**9. Heat resistant**
Provided by	Maltha Recycling	Maltha Recycling	Coolrec
Cullet size	≈1-3mm	≈3-10mm	≈3-20mm
			
Cullet contamination	ii) Float glass from various companies. iii. a,b) Minor traces of cardboard, sand, dust, plastic foil.	i) Fritting. ii) Various different tints, float glass from various companies. iii. a,b) Sand, dust, paper.	i) Fritting. ii) Float glass from various companies.

Container glass			
Type	**10. Clear**	**11. Clear**	**12. Green**
Provided by	Maltha Recycling	Sibelco	Sibelco
Cullet size	≈4-20mm	≈2-3mm	≈2-10mm
			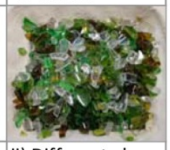
Cullet contamination	ii) Different glass producers, colours. iii. a, b, e) Paper, sand.	ii) Different glass producers, colours. iii. b, c) Sand, metal	ii) Different glass producers, colours

Figure 1. List of studied glass samples.

X-Ray Fluorescent (XRF) analysis was conducted in a selection of studied coatings, to identify the key elements to be introduced to the glass matrix during recycling. Also clear and tinted float glass samples were analyzed. Figure 2 presents the XRF results:

Float (non-tin side)		Float (non-tin side)		Soft coating (dark)*		Hard coating*	
Sample 1. IFS-SGT		Pilkington		Sample 3. Pilkington		Sample 4. Pilkington	
SiO2	74.167	SiO2	74.432	SiO2	64.665	SiO2	49.967
Na2O	12.52	Na2O	12.524	ZnO	14.703	SnO2	32.384
CaO	7.63	CaO	8.23	CaO	9.253	CaO	14.241
MgO	3.984	MgO	3.884	Na2O	4.736	MgO	1.153
SnO2	1.014	Al2O3	0.55	SnO2	2.732	Na2O	0.577
Al2O3	0.355	K2O	0.145	MgO	2.273	K2O	0.453
K2O	0.099	SO3	0.113	Al2O3	0.549	Fe2O3	0.35
Fe2O3	0.086	Fe2O3	0.057	TiO2	0.364	Al2O3	0.317
S	0.058	Traces: TiO2, SrO, P2O5, ZrO2, MnO, ZnO		S	0.171	S	0.237
Traces: Cl, TiO2, BaO, P2O5, ZrO2, SrO				ZrO2	0.163	TiO2	0.154
				K2O	0.16	Cl	0.069
				Fe2O3	0.094	ZrO2	0.055
				Traces: Ag2O, NiO, SrO, Cr2O3, P2O5, MnO		Traces: ZnO, Rb2O, P2O5	

Mirror 1, reflective coating*		Mirror 1, dialectric coating*		Mirror 2, reflective coating*		Mirror 2, dialectric coating*	
Sample 5		Sample 5		Sample 6		Sample 6	
SiO2	35.952	SiO2	19.756	CaO	39.435	BaO	21.544
CaO	26.887	BaO	19.667	SiO2	24.627	CaO	18.31
Na2O	13.893	ZnO	17.658	ZnO	23.766	SiO2	18.205
ZnO	10.907	MgO	11.331	MgO	6.777	TiO2	12.311
MgO	7.035	S	8.623	Fe2O3	3.832	MgO	8.399
Fe2O3	2.735	CaO	8.003	Al2O3	0.436	S	7.82
Al2O3	1.383	TiO2	7.272	S	0.421	ZnO	7.782
SO3	0.29	Al2O3	3.038	Ag	0.248	Fe2O3	3.824
P2O5	0.214	Fe2O3	2.362	TiO2	0.12	Al2O3	0.909
Ag2O	0.192	Er2O3	1.007	ZrO2	0.092	Na2O	0.26
TiO2	0.188	Co3O4	0.285	SnO2	0.08	K2O	0.121
PbO	0.101	Cl	0.247	Cl	0.056	Ag	0.107
K2O	0.088	Gd2O3	0.17	Traces: SrO, Cr2O3, K2O, P2O5		SrO	0.091
Traces: MnO, Cl, SrO, ZrO2		P2O5	0.104			Cr2O3	0.08
		Ag2O	0.103			P2O5	0.056
		Lu2O3	0.099			NiO	0.051
		SrO	0.09			Traces: ZrO2, Cl, SnO2, CuO	
		PbO	0.068				
		Traces: CuO, ZrO2, K2O, Br					

Float tint		Float opaque black coating*		Heat resistant opaque black frit*		Heat resistant white frit*	
Sample 8. Maltha		Sample 8. Maltha		Sample 9. Coolrec		Sample 9. Coolrec	
SiO2	71.846	SiO2	71.688	SiO2	33.171	SiO2	66.818
Na2O	12.452	Na2O	12.257	Cr2O3	22.493	Na2O	12.128
CaO	8.722	CaO	9.075	PbO	12.745	CaO	7.749
MgO	3.635	MgO	3.521	CuO	10.613	TiO2	6.966
Fe2O3	1.949	Fe2O3	2.006	Na2O	7.193	MgO	3.162
Al2O3	0.794	Al2O3	0.888	Fe2O3	3.802	Al2O3	1.487
K2O	0.303	K2O	0.28	Al2O3	3.565	K2O	0.565
S	0.142	S	0.146	CdO	2.939	ZrO2	0.499
TiO2	0.073	TiO2	0.058	TiO2	2.234	ZnO	0.207
Traces: Cl, MnO, P2O5, ZnO, SrO		Traces: MnO, NiO, ZnO, P205, SrO		CaO	0.347	S	0.181
				ZrO2	0.344	P2O5	0.096
				S	0.246	Fe2O3	0.087
				MgO	0.146	Traces: Cl, SrO, Rb2O	
				Traces: P2O5, Cl, SrO, Rb2O			

All compounds below 0.05% weight percentage are noted as traces
* The absolute Wt% are not entirely accurate in the case of thin coatings, due to the extremely small thickness of the coating.

Figure 2. Composition of selected glasses and coatings. XRF measurements conducted with a Panalytical Axios Max WD-XRF spectrometer.

All samples were kiln-cast at 1120°C for 10h, and then quenched and annealed at 560°C for 10h, employing a ROHDE ELS 200S kiln. Disposable investment moulds made from Crystalcast M248 were used in order to produce the cubic 50 mm specimens. The cullet was positioned inside the mould either in a structured or random manner (Fig 1).

An overview of the cast samples and their corresponding type of defects are presented in Figure 3.

Float glass			
Type	**1. Fully tempered**	**2. Low-iron**	**3. Soft-coating**
Kilncast sample at 1120°C	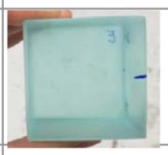		
A. Crystalline inclusions	-	-	-
B. Glassy inhomogeneities	-	-	Subtle
C. Bubbles	Miniscule	Miniscule	Miniscule
Type	**4. Hard-coating**	**5. Mirror 1**	**6. Mirror 2**
Kilncast sample at 1120°C		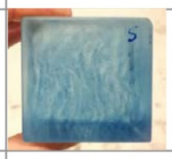	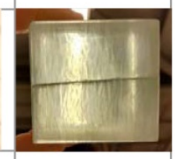
A. Crystalline inclusions	-	-	-
B. Glassy inhomogeneities	Subtle	Vertical (according to the positioning of the mirrors inside the mould)	Vertical (according to the positioning of the mirrors inside the mould)
C. Bubbles	Miniscule	Miniscule	Miniscule
Type	**7. Auto windshield**	**8. Tint, coat, clear**	**9. Heat resistant**
Kilncast sample at 1120°C	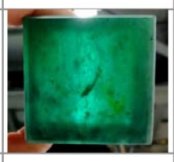	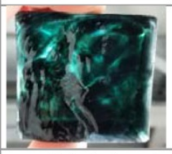	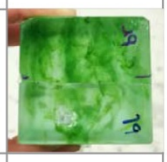
A. Crystalline inclusions	Yes	Possibly, induced by the frit	-
B. Glassy inhomogeneities	Yes	Yes	Yes
C. Bubbles	Miniscule	Miniscule	Miniscule

Container glass			
Type	**10. Clear (Maltha)**	**11. Clear (Sibelco)**	**12. Green**
Kilncast sample at 1120°C	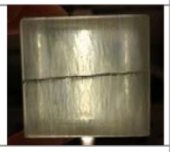		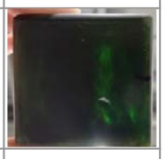
A. Crystalline inclusions	-	Yes, ceramic and metal inclusions	Yes
B. Glassy inhomogeneities	Yes	Yes	Yes
C. Bubbles	Miniscule	High content	Miniscule

Figure 3. Defects observed in the cast glass samples. (Note: The fragmented samples correspond to later tested specimens)

Assessing the above tested samples according to the defect categorization introduced in section 2.1, the following observations can be made:

A. Crystalline inclusions

Although this type of defect was not observed in the samples produced with clean glass from one source (no. 1-6), all other specimens kilncast using cullet provided by recycling companies had inclusions. These inclusions can be grouped as:

– A1. Inclusions from sand/stone/ceramics:

Mostly ceramic inclusions of max. 2mm diameter were observed in samples no. 7-12. These are linked to sand, stone and ceramic contamination in the cullet. They are tolerable within the glass matrix due to their small size.

– A2. Metal inclusions:

Linear metallic inclusions that did not exceed a diameter of 1mm and were non-disruptive. Observed in samples series 11.

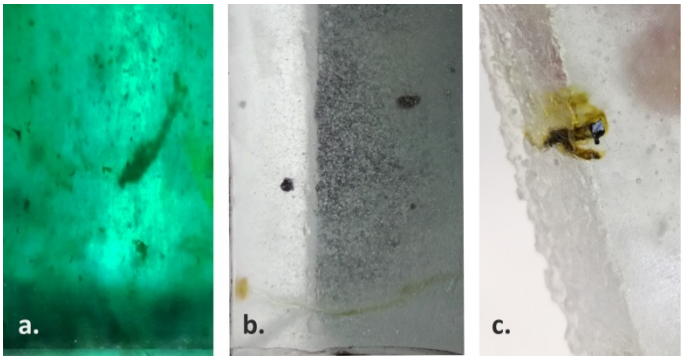

Figure 4. Crystalline inclusions observed in the cast specimens: a) Sample no. 7, defect A1. b) Sample no. 11, defect A1. c) Sample no. 11, defect A2.

B. Glassy inhomogeneities

– B1. Cord/ream

Samples series 5-12 presented evident glassy inhomogeneities, either due to the presence of coatings (no. 5-9), or due to minor compositional variations caused by the combination of tinted and clear soda-lime glasses from different manufacturers (no. 7-12). Subtle inhomogeneities due to coatings are also found in samples no. 3-4. Since the chosen casting viscosity is relatively high and no mechanical stirring was used, initial inhomogeneities in the cullet are traced in the final product. The size and shape of the cullet influence the level of homogenization and the shape of the observed cord and ream. None of the samples fractured during cooling due to the presence of such defects. To further investigate the level of inhomogeneities and their influence to the mechanical properties of the specimens, a selection of samples is tested via a Siemens Somatom Volume Zoom Computer Tomography (CT) scanner to identify density gradients, and with an Ilis StrainScope Flex polariscope to study the induced internal stresses.

The CT scanner tests show that the use of fine cullet results in localized density differentials (Fig. 6, white corresponds to higher density) while coarser cullet results in cords of denser material within the matrix (Fig. 5). The larger the cullet pieces and the more organized their positioning is in the mould, the more structured the cord will be. The circular polarization measurements taken with the Ilis StrainScope Flex show the existence of detectable stress along the glass and cord interface, yet the exact value cannot be quantified.

– B2. Frit inclusions:

Frits are finely powdered glasses that upon heating will form an either vitreous or devitrifying coating (Morena 2015), according to their composition and heat treatment. Traces from incompletely molten

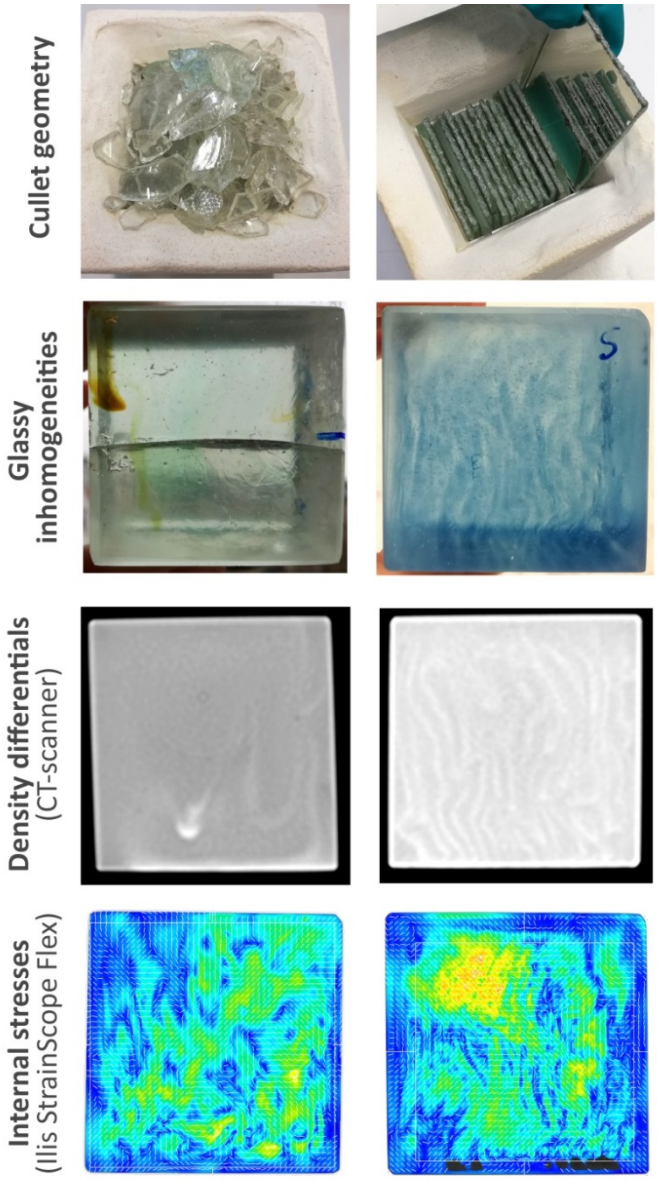

Figure 5. Glassy inhomogeneities as these resulted from 1) a variety of different soda-lime glasses: left column, sample no. 10, and 2) a metallic coating: right column, sample no.5. In the CT-scan images, white colour corresponds to higher density.

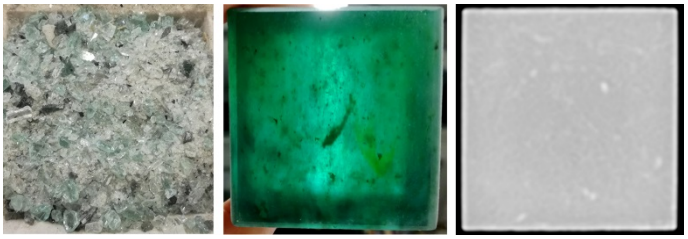

Figure 6. Glassy inhomogeneities in samples no.7. Relation of the density gradient as seen at the CT-scan (right) to the cullet size and contamination (left).

frit material were observed in samples no. 8-9. These dark-coloured non-spherical minuscule inclusions are organized in 3D “veils” that partially retain the planar geometry or even pattern of the initial frit-

ted surface. In the case of sample 9, the X-ray diffraction (XRD) analysis has not identified crystalline material. This could mean that indeed these inclusions are amorphous, or that their percentage is less than 1 wt% and cannot be traced by the test. Thus these inclusions are for the purposes of this paper classified under the "Glassy inhomogeneities" category, yet further research should be conducted to verify the absence of crystallinity. The XRF analysis of the "black frit" (Fig. 2, sample 9) - which seems to be associated with these inclusions - indicates a relatively thick layer of coating (the % of SiO_2, Na_2O and CaO corresponding to the glass below is low), of a composition rich in metal oxides. The composition suggests that a powdered natural mineral was used in the frit, and PbO was added to reduce the melting temperature. The Cr_2O_3, Al_2O_3 and TiO_2 compounds in the frit have high melting temperatures (2435°C, 2030°C and 1855°C respectively, NIH Database) which could explain its impartial melting and the presence of suspended material in the glass matrix which was not readily incorporable. The minuscule size of these defects (≥0.1mm) does not per se induce local stress to the matrix. However, the quantity of these inclusions and the density of their appearance introduces zones in the matrix, which although tolerable, seem to be disruptive to the glass network (see section 3.2).

– B3. Different glass types:

The presence of such contaminants would lead to cracking during cooling, due to their different thermal expansion coefficient to the glass matrix. This was mainly observed in samples series 10, and at a less extent in samples 9. XRD analysis in a sample from series 10 did not identify crystalline material/glass ceramic, thus linking the crack to the presence of a different glass type in the cullet.

Figure 7. a) Glassy inhomogeneities (B2) due to the heat-resistant frit in sample 9. b) Sample 8, incompletely molten frit, retaining the pattern of the initial coating. c) Presence of different glass type in sample 10, leading to cracking (B3).

C. Gaseous inhomogeneities

All samples presented minuscule bubbles. In general, the finer the cullet the higher the number of bubbles (e.g. series 7, 11). In the coated sample series 3-6, where the cullet was vertically organized inside the moulds, minuscule bubbles seem to cluster along 3D "veils" that form in proximity to the original vertical positioning of the coating. The clustering of bubbles along the reams is also observed in more randomly organized samples (e.g. series 10).

Figure 8. Bubble content increases with the decrease of cullet size. From left to right, samples no. 1, 10 and 11.

3 SPLITTING EXPERIMENTS

3.1 *Test set up*

A selection of specimens is further tested via a destructive splitting test. The set-up comprises a High-Speed Steel 10% Cobalt (HSS Co 10) tool bit of 25mm square cross section, rotated by 45° and positioned on a 52.4 hardened steel base, fixed on the base of a Zwick Z100 displacement controlled universal testing machine. The cubic glass specimens are centrally attached under the machine's steel head, which moves downwards with a 0.2mm/min rate. The slightly rounded top edge of the tool bit imposes a linear force along the middle of the bottom glass surface that eventually splits the specimen in two pieces (Figure 9).

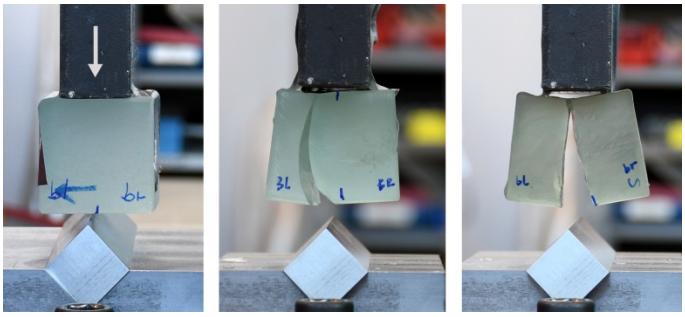

Figure 9. Left: splitting test set up. Middle: sample 6iii. Right: sample 10ii. The meso-structure of the specimens seems to affect the path of the crack.

3.2 *Results*

An overview of the tested samples and results can be found in figure 10. The number of results is limited and thus only indicative. The container glass cullet sample series (10, 11) seem to perform better than the float variants. Yet, series 3 failed at the highest and at some of the lowest values. In these specific specimens, the force was applied in parallel to the repetitive veils of glassy inhomogeneities and clustered inclusions. A low splitting stress could be linked to the proximity of the force line to one of the

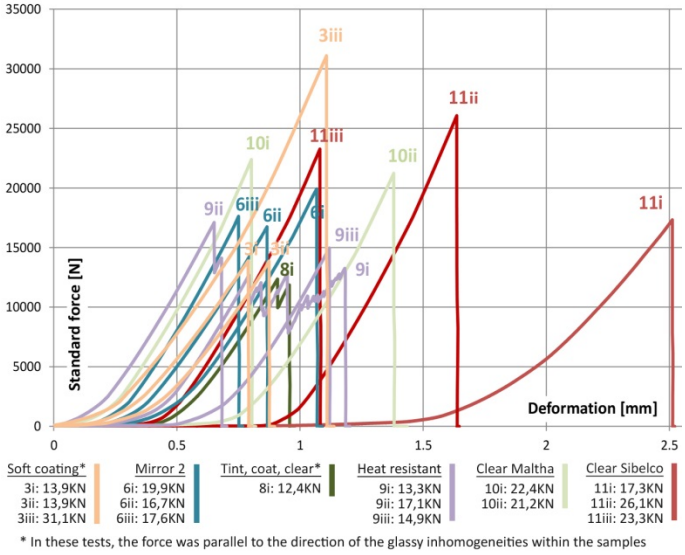

Figure 10. Splitting test results: force versus deformation graph

veil structures, hinting at orthotropy in the material properties. In other samples, where these parallel veils are perpendicular to the force direction (series 6, 9-11), the crack seems to slightly deviate when crossing these zones (Fig. 11). Series 11, which had the highest content of minuscule evenly distributed bubbles, also showed a wider range of failure values, and overall higher deformation than other samples. Samples 8 and 9, that contained a high amount of inhomogeneities from tints and frit, presented a lower failure strength average.

Figure 11. Side view of samples 10ii (left) and 11ii (right), showing the upward direction of the force and the -perpendicular to the force- zones of inhomogeneities.

4 CONCLUSIONS

In the majority of the cases the occurring inhomogeneities and inclusions were tolerated by the glass network during annealing. This is encouraging, given the fact that relatively low temperatures were used for the casting, thus the amount of expected defects is significantly higher than in the case of industrial casting at higher temperatures and lower viscosities. Nonetheless, the splitting tests showed that the high concentration of defects would decrease the splitting stress of the cubes. These defects were linked to the presence of coatings, recipe variations, or/and external contaminants in the cullet. Especially interesting is the case of recycled coated/fritted float glass, where 3D veils containing glassy zones and clustered minuscule bubbles and other non-spherical inclusions result from the incomplete incorporation of the coating to the glass matrix. This is particularly evident when the shape and positioning of the cullet inside the mould is structured prior to kiln-casting. Such organization can result in a more defined meso-structure that induces ortotrophy to the glass component, which may degrade its structural performance in the longitudinal direction. In the case of randomly shaped coated glass cullet, such distribution of defects is also incidental and more difficult to trace during inspection. This implies the development of a random global weakening of the glass network that will result in a lower failure strength. However, the recyclability of any type of coated/tinted float glass for structural purposes is not necessarily cancelled by the above fact. It only highlights the importance of awareness and the necessity of prototyping and mechanical testing prior to any structural application.

ACKNOWLEDGEMENTS

The authors would like to thank Hans van Limpt & Bart Wilms (Sibelco), Bianca Lambrechts & Danny Timmers (Maltha), Cor Wittekoek (Vlakglasrecycling), Brian Wittekoek (Coolrec), and Martijn Rietveld (NSG Pilkington), for their valuable input and waste glass supply. We are also very grateful to Henning Katte & Daniel Schreinert (Ilis) for sponsoring the use of StrainScope Flex. The contribution of Rong Yu & Tommaso Venturini (TU Delft Glass Lab) is also greatly acknowledged. We would also like to thank Ruud Hendrikx (TU Delft 3Me) for the XRF and XRD analyses, and Ellen Meijvogel-de Koning for the CT scanner measurements. Finally, a special thank you to Erik Muijsenberg (Glass Service) for supporting our work and vision.

REFERENCES

Bartuška, M.: Glass Defects Glass Service Inc. and Práh, Prague (2008)

Bristogianni, T., Oikonomopoulou, F., Justino de Lima, C., Veer, F.A., & Nijsse, R.: Structural cast glass components manufactured from waste glass: Diverting everyday discarded glass from the landfill to the building industry. HERON 63(1/2) (2018)

Glass Alliance Europe: Main glass sectors. www.glassallianceeurope.eu (2018).

Morena, R.: Frits and Sealing. Corning. (2015).

NHI, National Center for Biotechnology Information: PubChem Compound Database

Oikonomopoulou, F., Bristogianni, T., Veer, F., & Nijsse, R. : The construction of the Crystal Houses façade: challenges and innovations. Glass Structures & Engineering, (2017).

Rodriguez Vieitez, E., Eder, P., Villanueva, A., & Saveyn, H.: End-of-Waste Criteria for Glass Cullet: Technical Proposals. (2019)

TU Delft: Re3 Glass. Available: https://bit.ly/2u5tFgh. (2018)